REGULAR ARTICLE

Picric acid sensing and CO_2 capture by a sterically encumbered azo-linked fluorescent triphenylbenzene based covalent organic polymer

DHANANJAYAN KALEESWARAN and RAMASWAMY MURUGAVEL[*]

Department of Chemistry, Indian Institute of Technology Bombay, Powai, Mumbai, Maharashtra 400 076, India
E-mail: rmv@chem.iitb.ac.in

Abstract. A sterically encumbered isopropyl group substituted fluorescent triphenylbenzene based azo-linked covalent organic polymer, ^{i}PrTAPB-Azo-COP, has been synthesized by Cu(I) catalysed homo coupling (amine-amine) reaction of 1,3,5-tris(4′-amino-3′, 5′-isopropylphenyl)benzene (^{i}PrTAPB) under aerobic conditions. The Brunauer-Emmett-Teller (BET) and Langmuir surface areas of ^{i}PrTAPB-Azo-COP have been estimated to be 395 and 697 m^2 g^{-1} with a pore diameter of 11.6 Å. Due to the presence of fluorescent triphenylbenzene platform ^{i}PrTAPB-Azo-COP exhibits broad emission band centred at 428 nm, when excited at 300 nm, as a result of extended conjugation. The inherent fluorescent nature of ^{i}PrTAPB-Azo-COP has been utilized for sensing electron-deficient polynitroaromatic compounds (PNACs) such as a picric acid (PA), dinitrotoluene (DNT), *p*-dinitrobenzene (*p*-DNB) and *m*-dinitrobenzene (*m*-DNB). Further, ^{i}PrTAPB-Azo-COP has also been utilized for capture of carbon dioxide as the azo-COP is enriched with CO_2-philic nitrogen atoms apart from its microporosity. Since the azo (–N=N-) linkages are masked by the bulky isopropyl groups, ^{i}PrTAPB-Azo-COP exhibits a CO_2 uptake of 6.5 and 19.4 wt% at 1 bar and 30 bar, respectively, at 273 K.

Keywords. Azo linkage; COPs; CO_2 capture; nitroaromatic sensing; triphenylbenzene.

1. Introduction

The growth of fine chemical industries such as dye, leather, pesticide and pharmaceutical industries results in increased contamination agricultural lands and water bodies by chemical wastes.[1] One of the extensively used chemicals in these industries is 2,4,6-trinitrophenol (picric acid, PA). PA has been demonstrated to be a potential threat to human health as it damages the liver function and respiratory systems.[2] It has also been found to be responsible for anaemia, cancer, infertility, gastritis, sycosis, diarrhoea and skin and eye irritation.[3] More importantly, PA has been recognized as a common and potential explosive as compared to other polynitroaromatic compounds (PNACs) such as trinitrotoluene (TNT), *p*-dinitrobenzene (*p*-DNB), *m*-dinitrobenzene (*m*-DNB), dinitrotoluene (DNT), *etc.*, due to the low safety coefficient and high explosion energy.[1,4] It has been observed that the explosion power of PA is much higher than that of the other powerful

congener TNT.[1,5] Hence, it is an important and urgent need to address this exigent issue by developing sensitive and selective detection method to monitor the trace levels of PA in the environment. Optical methods, especially fluorescence-based detection methods,[6] could be a promising solution for the detection of PA compared to other conventional detection methods (trained canines, metal detectors, gas chromatography coupled with mass spectrometry (GC-MS), electrochemistry, ion mobility spectroscopy (IMS), colorimetry, quartz crystal microbalance (QCM), surface enhanced Raman spectroscopy (SERS) and so on).[7] Fluorescence detection methods have become popular due to short response time, real-time usage, low cost with high sensitivity, high selectivity, simple and portable to on-site for detection.[8]

In this regard, many fluorescence-based organic (small molecules/polymers), inorganic and organic-inorganic hybrid materials such as pyrene,[9] anthracene,[10] boron compounds,[1,11] luminescent gels,[12] dendrimers,[13] carbazole derivatives,[14] fluoranthene,[8,15]

quantum dots,[16] polyhedral oligomeric silsesquioxane (POSS),[17] metal-organic cages,[18] metal-organic frameworks (MOFs),[19] covalent organic frameworks (COFs),[20] molecularly imprinted polymers (MIPs),[21] covalent organic polymers (COPs)[9,14,22] have been utilized for the detection of PNACs. Among these materials, COPs have gained much attention for many reasons.[22] Firstly, while comparing with the small organic molecules or fluorophores, COPs are outstanding electron donors because of the extended π-conjugation. Further, the donor ability of the COPs is enhanced in the excited state due to the delocalized π* state, which offers a platform for the easy migration of excitons. As a result, the interaction between the COPs and PNACs will increase and the fluorescence intensity will be quenched. This phenomenon is known as 'molecular wire effect,' coined by Swager *et al.*,[5,23] Secondly, the COPs have been constructed through either C-C bonds or C-N bonds, offering excellent stability under harsh conditions (e.g., acidic or basic medium).[9] Besides, the structure and porosity of COPs can be fine-tuned by judicious selection of fluorescent monomers since high porosity or pore size will tend to increase the diffusion of PNACs into the porous polymer network and hence increase the fluorescence quenching efficiency.[14]

Apart from detection of PNACs, COPs have been known for their gas storage and separation (e.g., carbon dioxide (CO_2) capture[24]) owing to their intrinsic porosity. The other potential applications of COPs lie in the areas of catalysis, drug delivery, clean energy storage, semiconductors and optoelectronic devices.[25] The main advantage of COPs as CO_2 capture material is their reusability due to the interaction between the CO_2 and COPs is considered to be weak. The conventional industrial amine scrubbing method employs aqueous amine solutions (monoethanolamine (MEA) or diethanolamine (DEA)) which react with CO_2 to produce carbamates. Corrosive nature of the amine solutions and the necessity of high energy for regeneration makes this method very cumbersome and expensive.[26] Hence, COPs are superior materials for the capture of CO_2. Further, CO_2 uptake can be enhanced by increasing CO_2-philic nitrogen functional groups (amine, azo, benzimidazole, imine, triazine, *etc.*) in the polymer networks,[27] either by proper choice of nitrogen-containing monomers or by post modification protocols.[28]

Recent research from our group has reiterated that the fluorescent small molecules,[14,29] and porous organic frameworks (COFs and COPs).[9,14,20] derived from triphenylbenzene, carbazole and π-extended pyrene monomers exhibit impressive detection ability towards PNACs by fluorescence quenching. Further, we have demonstrated that the presence of adequate CO_2-philic

nitrogen groups such as aminal, imine, azo, triazine linkages in the porous polymer networks would profoundly enhance the CO_2 uptake.[9,20,30] Keeping the above observations in mind, here we demonstrate how the presence of bulky isopropyl group in the ortho position to amine functionality in triphenylbenzene system can affect the azo-polymerization process, PNACs sensing ability and CO_2 uptake capacity.

2. Experimental

### 2.1 *Materials, methods and instruments*

All the reactions were carried under normal aerobic atmosphere conditions since both the starting materials and products were found to be moisture and air-stable. Solvents were purified according to standard procedures prior to their use.[31] Starting materials such as CuBr (Alfa Aesar), pyridine (Merck), 2,4-dinitrotoluene (Sigma-Aldrich), picric acid (Loba Chemie, India), *m*-dinitrobenzene (Thomas Baker, India) and *p*-dinitrobenzene (Spectrochem, India) were procured from commercial sources and used after crystallization from suitable solvents.

Caution: *Picric acid, p-DNB, m-DNB and DNT are sensitive to external stimuli such as shock, heat, electromagnetic radiation, static electricity, etc. Although we did not face any kind of difficulty while working with them, it is highly advisable to handle these materials with due care.*

The melting points were measured in open glass capillaries and are reported uncorrected. Infrared spectra were obtained on a Perkin–Elmer Spectrum One FT-IR spectrometer as discs diluted in KBr. Microanalyses were performed on a ThermoFinnigan (FLASH EA 1112) microanalyzer. NMR studies were performed on a Bruker Avance DPX-400 and 500 MHz spectrometers. CP-MAS ^{13}C NMR measurements were carried out on a Bruker Avance 500 MHz spectrometer at 300 K and the samples were packed in 4.0 mm zircon rotor. The ESI-MS studies were carried out on a Bruker MaXis impact mass spectrometer. Thermo gravimetric analyses were carried out on a Perkin–Elmer Pyris thermal analysis system under a stream of nitrogen gas at the heating rate of 10 °C/min. Powder X-ray diffraction measurements were recorded on a Philips X'pert Pro (PANalytical) diffractometer using Cu-Kα radiation (λ = 1.5419 Å). The absorption spectra were recorded on a Varian Cary Bio 100 UV-vis spectrophotometer. The fluorescence spectral studies were performed on a Varian Cary Eclipse fluorescence spectrophotometer equipped with a Xenon flash lamp light source and a 1 cm path length quartz cuvette.

2.2 *Adsorption measurements*

Adsorption measurements were carried out on a Quantachrome Autosorb-1C analyzer using UHP-grade N_2 and CO_2 gases, which were used as received without further
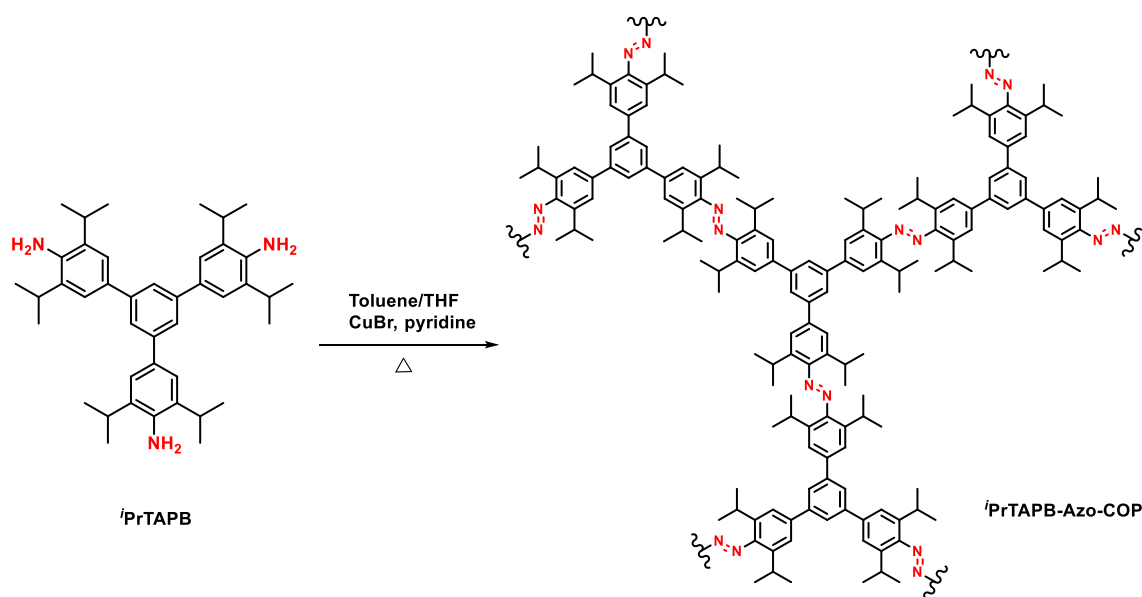
Scheme 1. Synthesis of ^{i}PrTAPB -Azo-COP.

purification. N$_2$ adsorption measurements were performed at 77 K on a liquid nitrogen bath. Adsorption measurements 273 and 298 K for CO$_2$ and N$_2$ were performed on a water-bath. All the adsorption measurements were done up to 1 bar. Prior to the measurements, the sample was evacuated at 120 °C for 5 h under ultrahigh vacuum in Autosorb-1C.

2.3   *FEG-SEM*

The morphology of ^{i}PrTAPB-Azo-COP was examined using field-emission gun-scanning electron microscopy (FEG-SEM) on a JEOL model JSM-7600F electron microscope, operating at the accelerating voltage of 0.1 to 30 kV. The sample was prepared by drop-casting the powdered sample onto the carbon substrate. The samples were sputtered with platinum prior to the imaging.

2.4   *FEG-TEM*

The TEM analysis of ^{i}PrTAPB-Azo-COP was investigated using high-resolution transmission electron microscope (Tecnai G2, F30) equipped with field emission source operating at 300 KeV to image the sample on a carbon coated copper TEM grids. The samples were prepared by dispersing the COP in acetone by sonication and drop-casted on the TEM grids. The samples were dried under an infrared lamp for 30 min before imaging experiments.

2.5   *Photophysical studies*

^{i}PrTAPB-Azo-COP (1.0 mg) was dispersed in acetonitrile (5 mL) and sonicated for 10 minutes to obtain a homogeneous dispersion. The absorption and fluorescence spectra of the ^{i}PrTAPB-Azo-COP were recorded at room temperature using 1 cm path length quartz cuvette. The fluorescence spectrum

of the suspension was measured by increasing addition of polynitroaromatic analytes, keeping an excitation and emission slit width of 10 nm. ^{i}PrTAPB-Azo-COP was excited at 300 nm. The fluorescence intensity (I) was plotted against wavelength to obtain quenching profiles. The values of the Stern–Volmer constant (K_{SV}) were calculated by fitting the fluorescence data to the following equation.

$$I_0/I = 1 + K_{sv}[Q] \tag{1}$$

where, I_0 = fluorescence intensity in the absence of the analyte, I = fluorescence intensity in the presence of the analyte, K_{SV} = Stern–Volmer constant, and [Q] = concentration of quencher/analyte. The Stern–Volmer curves were obtained by plotting (I_0/I) versus analyte concentration.

2.6   *Synthesis of ^{i}PrTAPB-Azo-COP*

^{i}PrTAPB (200 mg, 0.4 mmol) was stirred at room temperature for 48 h in the presence of pyridine and CuBr in toluene/THF (v/v) mixture. Then the reaction mixture was heated at 60 °C and 80 °C for 24 h each and 120 °C for 48 h. During the course of the reaction, the colour changed from colorless and eventually yielded a blood-red colored precipitate. The precipitate was filtered and washed with THF to remove the unreacted ^{i}PrTAPB. The precipitate was stirred in conc. HCl for 24 h followed by aq. NaOH (1M) for 24 h. Finally, the red precipitate was washed with water, ethanol and dried under vacuum for 12 h at 120 °C. Yield: 0.0680 g, 30%. M.p.> 300 °C. Anal. Calcd. for C$_{42}$H$_{51}$N$_3$: C, 84.37; H, 8.60; N, 7.03%. Found: C, 78.26; H, 5.63; N, 7.95%. FT-IR (KBr diluted disc); 3407, 2962, 2927, 1623, 1593, 1463, 1438, 1385, 1107, 1070 and 1020 cm^{-1}. CP-MAS ^{13}C NMR (δ, ppm): 147.4, 143.2, 138.8, 131.6, 122.6, 26.8 and 22.0.

3. Results and Discussion

3.1 *Synthesis and characterization*

The synthesis of monomer ^{i}PrTAPB, hexaisopropyl appended derivative of 1,3,5-tris(4′-aminophenyl) benzene (TAPB) is reported elsewhere.[20] The substitution of sterically encumbered bulky isopropyl groups on the TAPB increases the chemical stability (both in acids and bases) as well as the hydrophobicity of the resultant COP. Further, the presence of bulky isopropyl groups renders triphenylbenzene platform electron rich, and as a result, enhances the PNACs detection sensitivity and CO_2 adsorption with increased CO_2/N_2 selectivity by improving Lewis acid-base interactions.[9,27,32]
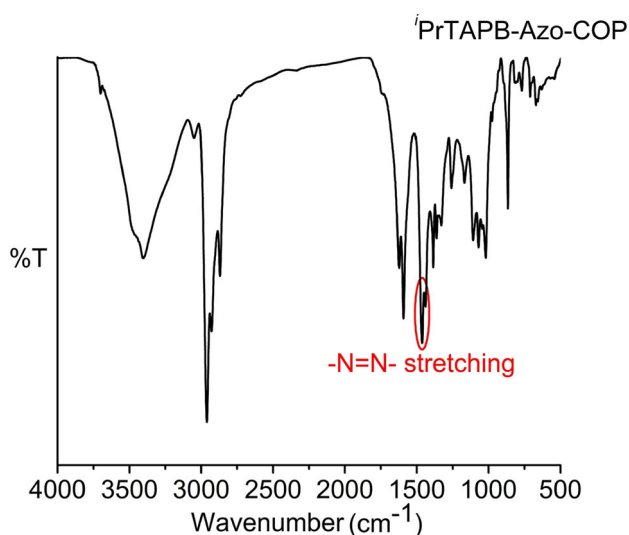

Figure 1. FT-IR spectrum of ^{i}PrTAPB-Azo-COP (as KBr disk).

The azo-COP, ^{i}PrTAPB-Azo-COP, has been synthesized by the homo amine-amine coupling reaction of ^{i}PrTAPB in THF / toluene solvent mixture. This reaction is catalysed by Cu(I) salt and catalytic amounts of pyridine in the air (oxygen).[27] In order to achieve complete polymerization, the temperature of the reaction has been increased from room temperature to 120 °C (Scheme 1). To minimize the undesired side reactions, the reaction has been carried out at ambient temperature for 48 h, and successively at 60 and 80 °C for 24 h each. Unlike other amines,[27,33] the -NH$_2$ group of ^{i}PrTAPB is flanked by two isopropyl groups and hence results in a reduced yield of the polymer at 80 °C. In order to ensure complete conversion, the temperature of the reaction was further increased to 120 °C for 48 h. The precipitated blood-red product was purified as noted in the experimental section. ^{i}PrTAPB-Azo-COP is insoluble in most organic solvents, e.g., acetone, acetonitrile, chloroform, dichloromethane, DMF, DMSO, THF, etc. More importantly, the azo-COP is stable in 4 M HCl and 4 M NaOH, as the work-up of the reaction involves strong acids and bases.

^{i}PrTAPB-Azo-COP has been unambiguously characterised by FT-IR, cross-polarized magic angle spinning (CP-MAS) ^{13}C NMR, thermogravimetric analysis (TGA), powder X-ray diffraction (PXRD), scanning electron microscopy (SEM), transmission electron microscopy (TEM) and analytical methods. Formation of azo linkage (-N=N-) is confirmed by the characteristic -N=N- stretching vibrational bands at 1463 and 1438 cm^{-1} in the FT-IR spectrum of ^{i}PrTAPB-Azo-COP (Figure 1). The bands at 2962 and 3050 cm^{-1} are attributed to the alkyl and aromatic C-H stretching vibrations. The
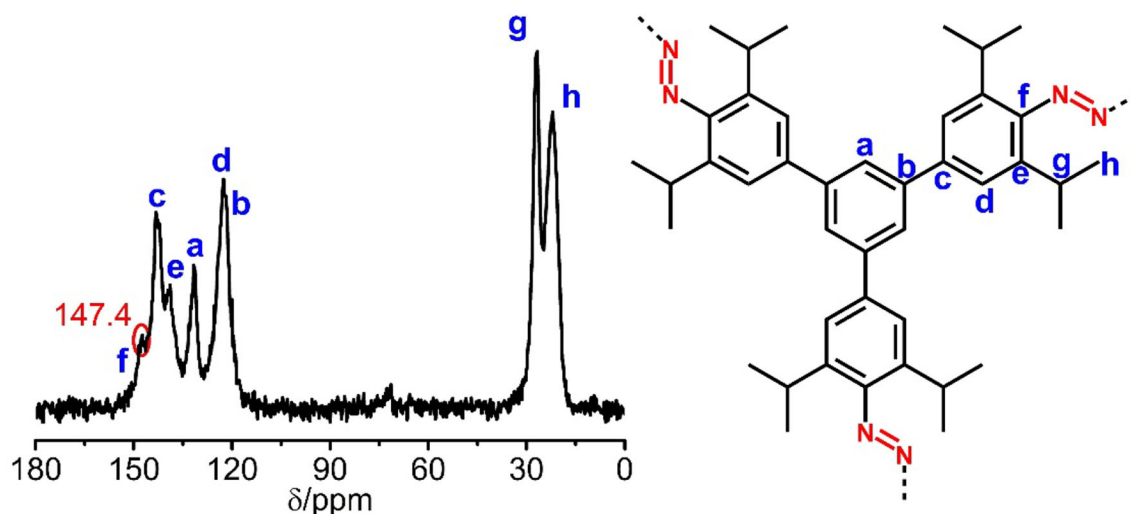

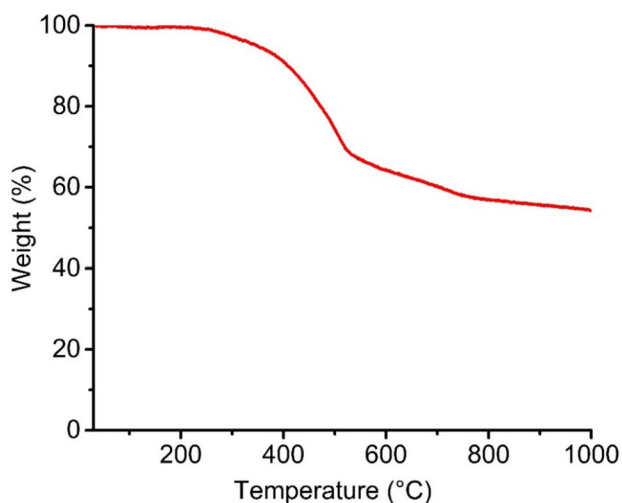**Figure 2.** CP-MAS ^{13}C NMR spectrum of ^{i}PrTAPB-Azo-COP.

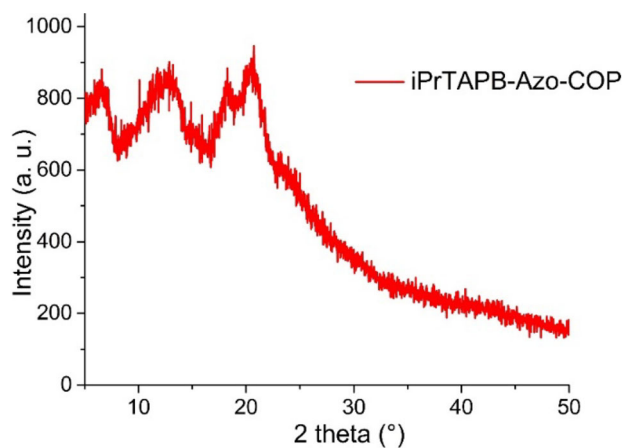**Figure 3.** TGA trace of ^{i}PrTAPB-Azo-COP at a heating rate of 10 °C per minute under the flow of nitrogen.

Figure 4. PXRD pattern of ^{i}PrTAPB-Azo-COP.

unreacted terminal –NH$_2$ groups exhibit a broad vibrational band at 3407 cm^{-1}.[9,27,33] To further confirm the formation of azo linkage, solid-state CP-MAS ^{13}C NMR spectrum of the ^{i}PrTAPB-Azo-COP was recorded. The resonance of carbons atom connected to the -N=N- linkage appears at 147 ppm (Figure 2). The resonances at 27 and 22 ppm correspond to the carbon atoms of isopropyl groups. The resonances in the range of 143–122 ppm are due to the other aromatic carbon atoms of the azo-COP.

The thermal stability of the ^{i}PrTAPB-Azo-COP was investigated by TGA of the activated solid sample under nitrogen at a heating rate of 10 °C/min. The TGA trace of the ^{i}PrTAPB-Azo-COP suggests that the polymer is stable up to 300 °C and the decomposition of the polymeric network starts after 300 °C (Figure 3). The stability of the ^{i}PrTAPB-Azo-COP is lower than ALP-4 which does not have any isopropyl group.[27] The broad PXRD pattern of azo-COP confirms the amorphous nature of the polymer (Figure 4). SEM analysis of the ^{i}PrTAPB-Azo-COP reveals uniformly distributed several hundred nanometer-sized particles with spherical morphology (Figure 5a). TEM image of the polymer shows a long ribbon-like structure with stacked layers (Figure 5b).

3.2 *Photophysical studies and PNACs detection*

As the polymer is insoluble in common organic solvents, absorption and emission studies were investigated by dispersing 1 mg of ^{i}PrTAPB-Azo-COP in acetonitrile by sonication for 10 minutes at room temperature. The absorption spectrum of ^{i}PrTAPB-Azo-COP exhibits three bands at 220, 265 and 358 nm which are attributable to $\pi - \pi*$ and n-$\pi*$ transitions (Figure 6a). Further, the band at 358 nm is characteristic for azo-functionality, which confirms the *trans*-orientation of phenyl rings with respect to azo-linkage.[27] The emission spectrum of ^{i}PrTAPB-Azo-COP exhibits a broad blue emission at 428 nm, which tails up to 540 nm,
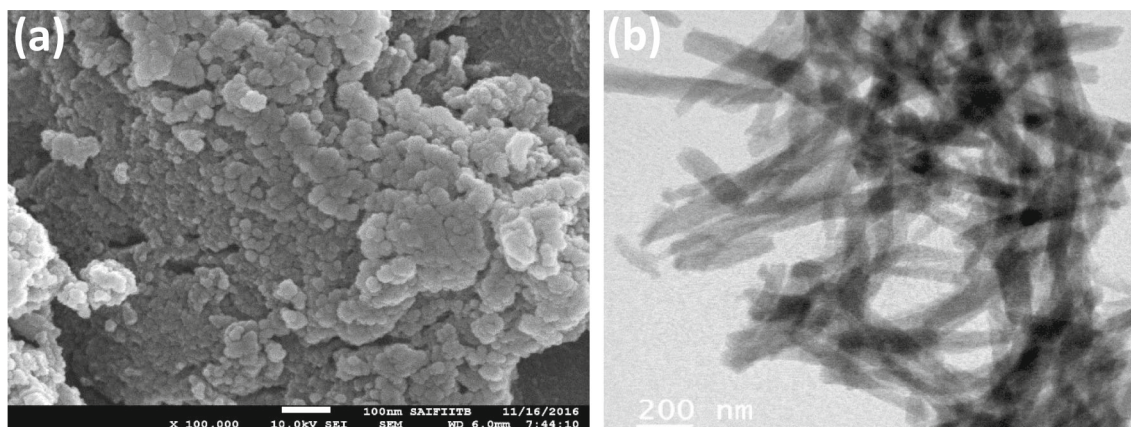

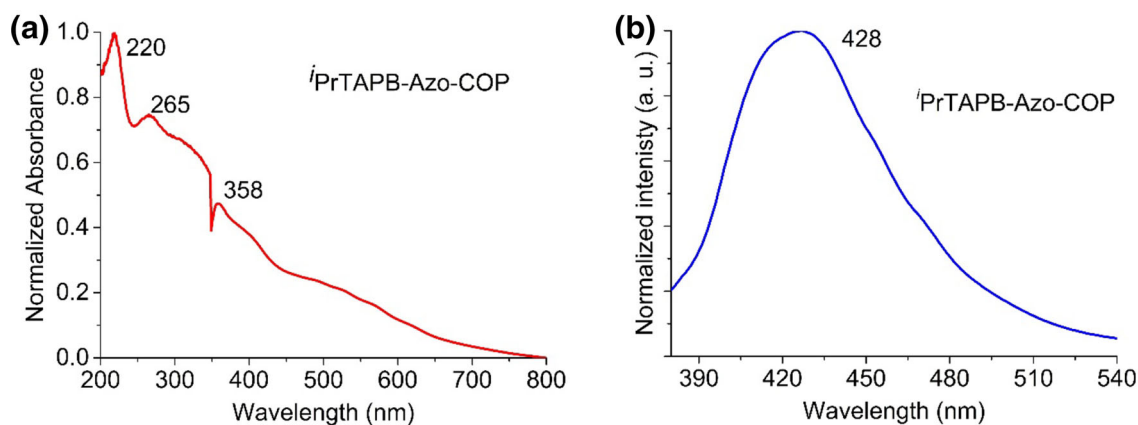**Figure 5.** (a) SEM and (b) TEM images of ^{i}PrTAPB-Azo-COP.

Figure 6.   (a) Absorption and (b) emission (λ_{ex} = 300 nm) spectra of dispersion of ^{i}PrTAPB-Azo-COP in acetonitrile.
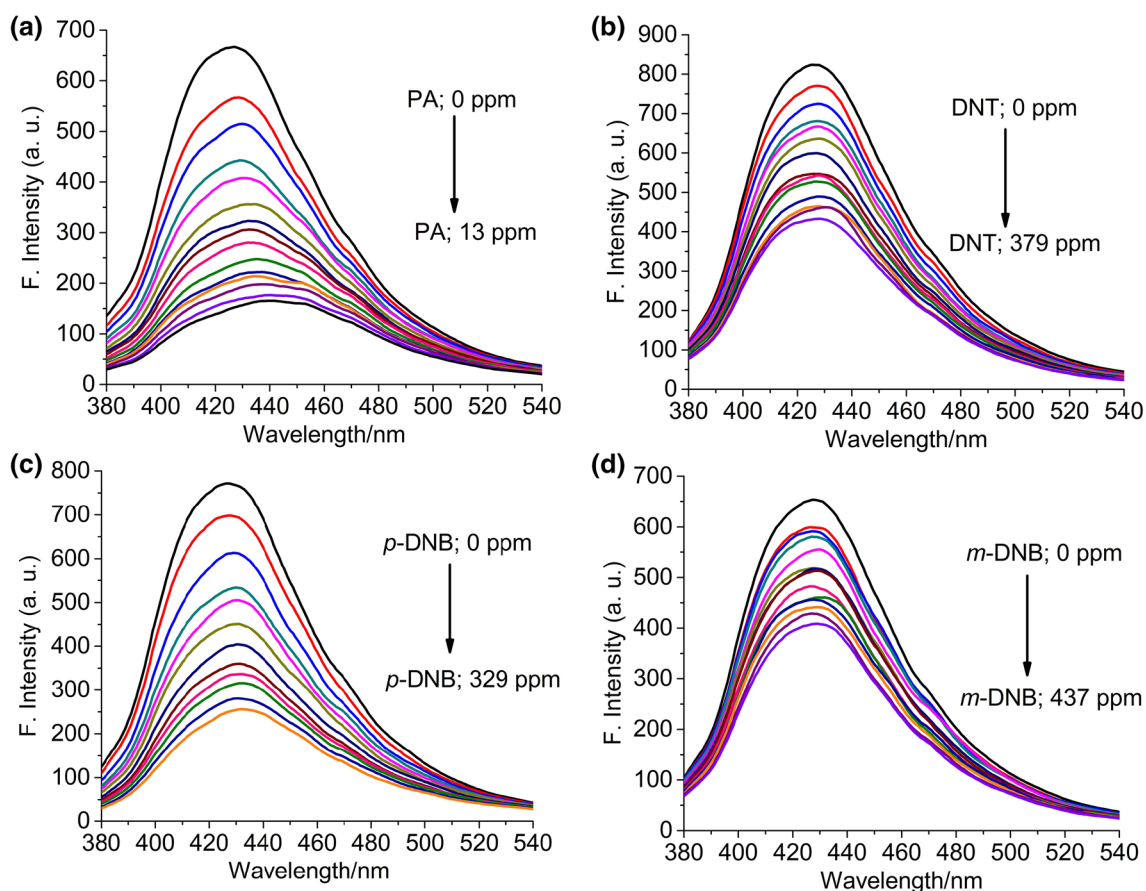

Figure 7.   Fluorescence quenching studies of ^{i}PrTAPB-Azo-COP using (a) PA; (b) DNT; (c) *p*-DNB and (d) *m*-DNB in acetonitrile (λ_{exci} = 300 nm).

when excited at 300 nm (Figure 6b). In comparison with the monomer (^{i}PrTAPB) emission wavelength (412 nm),[20] the polymer emission is red shifted by 16 nm due to the extended π-conjugation. Thus, the inherent fluorescent behaviour of triphenylbenzene moieties in ^{i}PrTAPB-Azo-COP paves the way for sensing of different electron deficient polynitroaromatic compounds

(PNACs) by quenching the fluorescent intensity of polymer.

In order to investigate the detection of PNACs, four different electron-deficient PNACs, picric acid (PA), dinitrotoluene (DNT), *p*-dinitrobenzene (*p*-DNB) and *m*-dinitrobenzene (*m*-DNB), were chosen as analytes. The fluorescence intensity of the ^{i}PrTAPB-Azo-COP
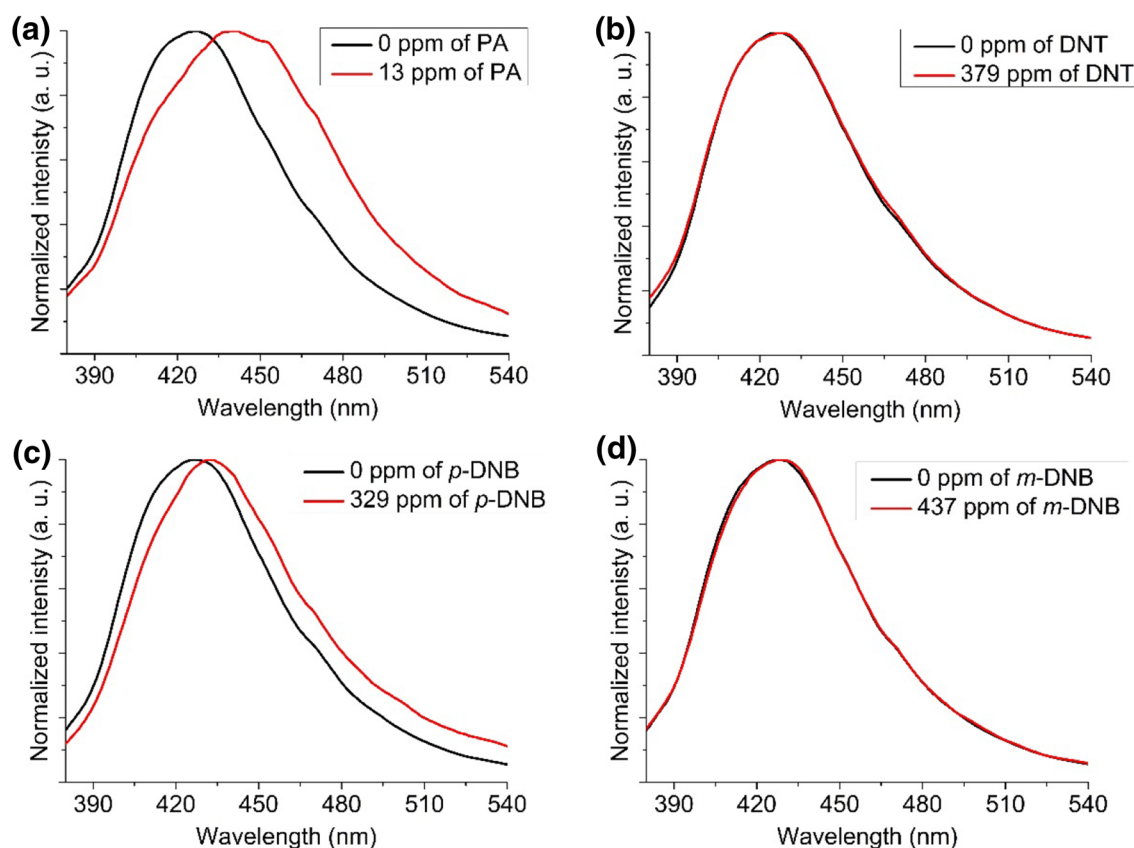
Figure 8. Change of ^{i}PrTAPB-Azo-COP fluorescence maximum before and after the addition of (a) PA; (b) DNT; (c) *p*-DNB and (d) *m*-DNB in acetonitrile (λ_{exci} = 300 nm).

has significantly diminished upon increasing the concentration of PNACs (Figure 7). Particularly, an abrupt change in fluorescence intensity was observed, almost 77% of quenching, by the addition of 13 ppm of PA (Figure 7a). This can be understood in terms of, (a) high electron deficiency of the PA due to the presence of three electron withdrawing nitro groups and (b) transfer of acidic –OH proton from PA to nitrogen atoms of azo-COP. As seen from Figure 8, the fluorescence intensity of PA is red shifted by 14 nm (428 to 442 nm) after the addition of 13 ppm of PA, confirming the transfer of PA proton to azo-COP.

This phenomenon has already been reported for other small molecular sensors as well as polymers.[20,29,34] These fluorescence studies suggest that ^{i}PrTAPB-Azo-COP is a better sensor for the PA, because other PNACs quench fluorescence only at higher concentrations (>350 ppm) that too with no observable shift in the fluorescence spectral maximum after the addition of the analytes (Figure 9). The extent of quenching by different analytes after the addition of 13 ppm of PNACs is illustrated in Figure 10 and Table 1.
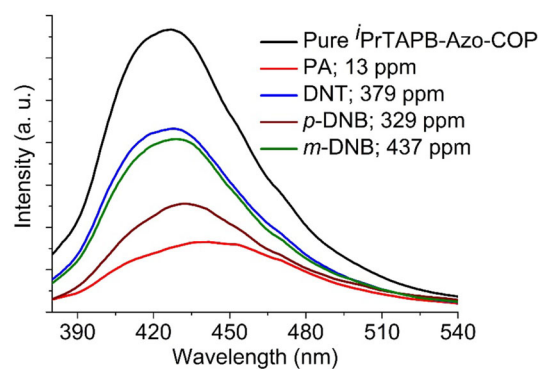

Figure 9. Combined fluorescence quenching profile of PNACs.

In order to evaluate the quenching efficiency of ^{i}PrTAPB-Azo-COP, Stern–Volmer plot was employed from the steady state fluorescence measurements (Figure 11) and the Stern-Volmer constants (K_{SV}) are presented in Table 1. The K_{SV} values for PA, DNT, *p*-DNB and *m*-DNB are calculated to be 1.1×10^4, 1.7×10^3, 4.3×10^3 and 8.9×10^1 M^{-1}, respectively. The order of quenching efficiency is PA $>>$ *p*-DNB $>$ DNT $>>$ *m*-DNB. The ratio of fluorescence intensity
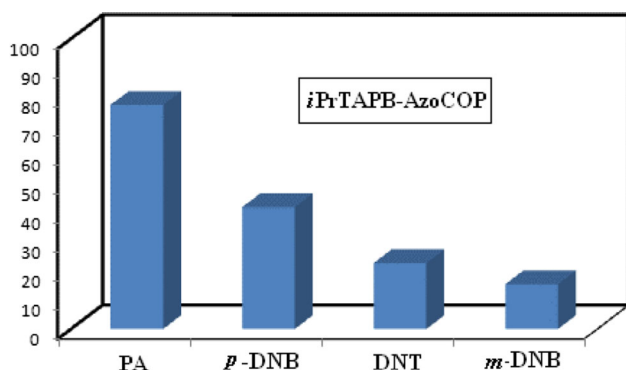
Figure 10. The degree of quenching upon addition of 13 ppm of polynitroaromatic compounds with ^{i}PrTAPB-Azo-COP.

Table 1. Quenching efficiencies for ^{i}PrTAPB-Azo-COP with different PNACs.

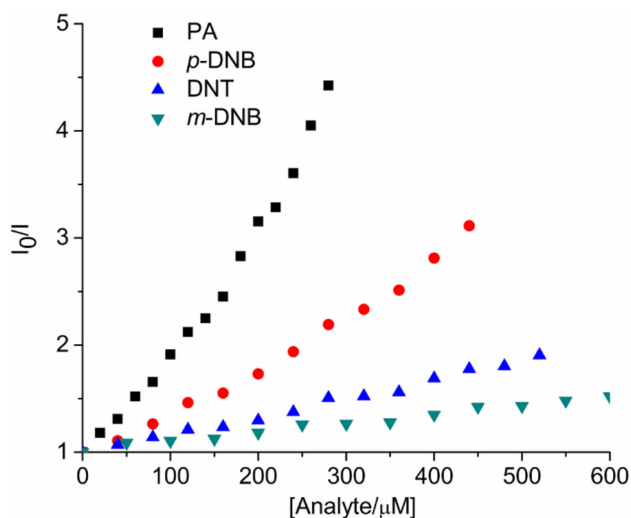| Analyte(s)	% Quenching	$K_{sv}(\mathbf{M^{-1}})$
PA	77	1.1×10^4
p-DNB	68	4.3×10^3
DNT	48	1.7×10^3
m-DNB	38	8.9×10^1

Figure 11. Stern–Volmer plots of ^{i}PrTAPB-Azo-COP with PNAC analytes.

against the concentration of PNACs follows linear or quasi-linear dependence (linear at low concentrations) and it is suggesting involvement of static quenching mechanism (Figure 11).

3.3 *Gas sorption studies*

To evaluate the surface area, pore diameter and pore size distribution of ^{i}PrTAPB-Azo-COP, nitrogen sorption was investigated at 77 K and 1 bar. The N_2 isotherm

of ^{i}PrTAPB-Azo-COP exhibits Type I isotherm with a sharp uptake of N_2 at low partial pressures (0.0–0.1 bar), indicating the presence of micropores in the polymeric network (Figure 12a). The hysteresis observed in the high and low-pressure regions suggest the swelling effect of the polymer at low temperature (77 K)[35] as well as the presence of some mesopores in ^{i}PrTAPB-Azo-COP.[9] The BET and Langmuir surface areas of ^{i}PrTAPB-Azo-COP was estimated to be 395 and 697 m^2g^{-1}, which is either comparable or even higher than the values observed for other azo-linked polymers (azo-COP-3, 388 m^2g^{-1};[27] Azo-POF-2, 435 m^2g^{-1};[32] Azo-MOP-4, 335 m^2g^{-1};[32] ALP-7 and NOP-34 @5050, 412 m^2g^{-1};[33,35] NOP-34 @3070, 397 m^2g^{-1};[35] Azo-CPP-7, 197 m^2g^{-1};[36] NOP-34 @0100, 245 m^2g^{-1};[35]). The observed values are however lower than a few other azo-COPs (Py-azo-COP, 700 m^2g^{-1}; ALP-1, 1235 m^2g^{-1}; ALP-2, 1065 m^2g^{-1}).[9,27] A complete list of surface area of azo-COPs is presented in Table S2 in SI. The pore size distribution (PSD) and pore diameter were calculated from Non-Local Density Functional Theory (NLDFT) method. The adsorption branch of the nitrogen isotherm was fitted to slit-pore model on carbon at 77 K. PSD study shows that ^{i}PrTAPB-Azo-COP has a major peak at 9.6 Å, confirming that the polymer essentially contains uniform pores in the framework, though a small hump appears in the mesopore range (37.0 Å) (Figure 12b). The pore volume of ^{i}PrTAPB-Azo-COP was evaluated from the nitrogen gas adsorbed at $P/P_0 =$ 0.99 to be 0.259 cc g^{-1}. The surface area, pore diameter and pore volume of ^{i}PrTAPB-Azo-COP were lower than unsubstituted variant ALP-4 (S_{BET} = 862m^2g^{-1}, pore diameter = 11.0 Å and pore volume = 0.50 cc g^{-1}).[27] due to the presence of bulky isopropyl groups. The nitrogen sorption measurement results suggest that the pores in the ^{i}PrTAPB-Azo-COP can be used for hosting various guest molecules and gases such as CO_2.

The presence of CO_2-philic nitrogen atoms in the form of azo linkages and the dominant micropores with few mesopores inspired us to investigate the CO_2 adsorption behaviour of ^{i}PrTAPB-Azo-COP. The CO_2 adsorption measurements were evaluated at two different temperatures (273 and 298 K) up to 1 bar. ^{i}PrTAPB-Azo-COP exhibits CO_2 uptake of 6.5 and 3.9 wt % at 273 and 298 K, respectively (Figure 13a). The CO_2 uptake values obtained are moderate as compared to the previously reported azo-linked polymers (Table S2, SI). The CO_2 isotherms exhibit completely reversible isotherms suggesting a weak interaction of CO_2 with the framework, suggesting facile regeneration of the material without any external stimuli. The azo-linked polymers synthesized from the flat aromatic platforms, without any pore blocking substituents in the
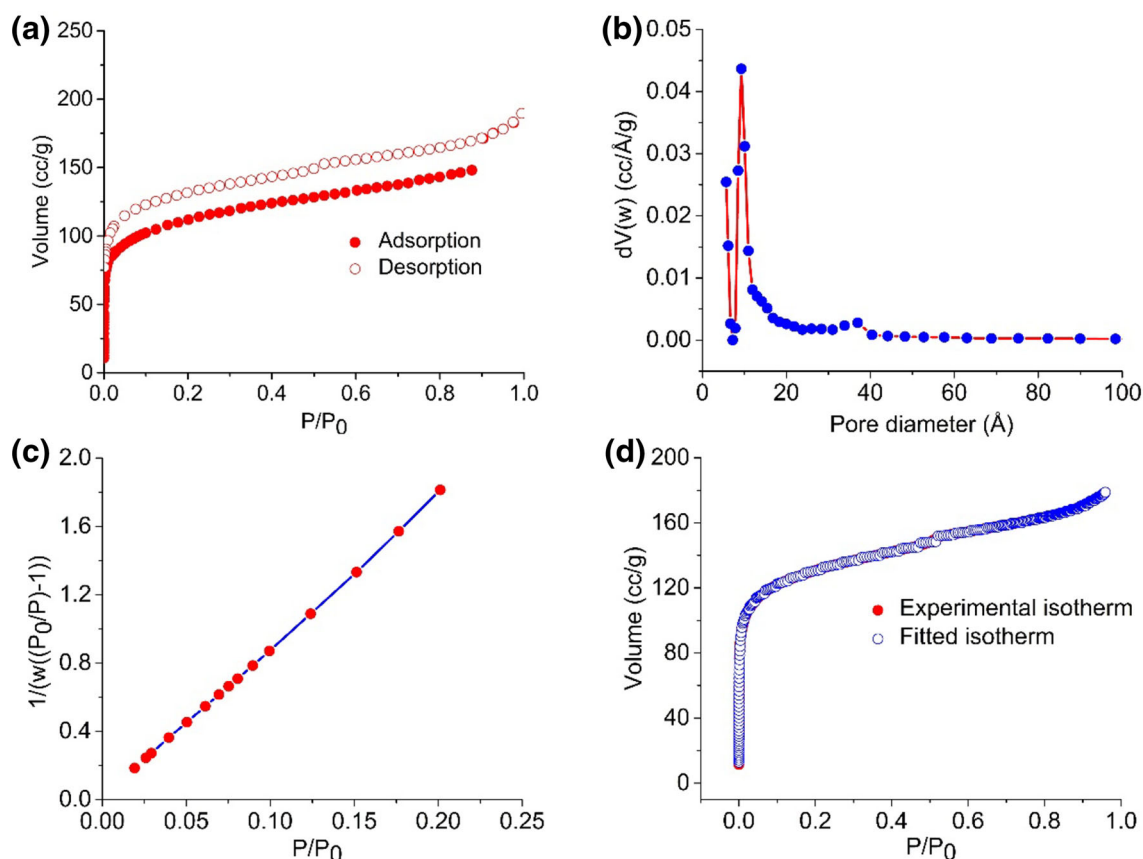
Figure 12. (a) Nitrogen sorption isotherm of ^{i}PrTAPB-Azo-COP at 77 K and 1 bar; (b) Pore size distribution profile; (c) BET plot and (d) NLDFT fitted isotherm.
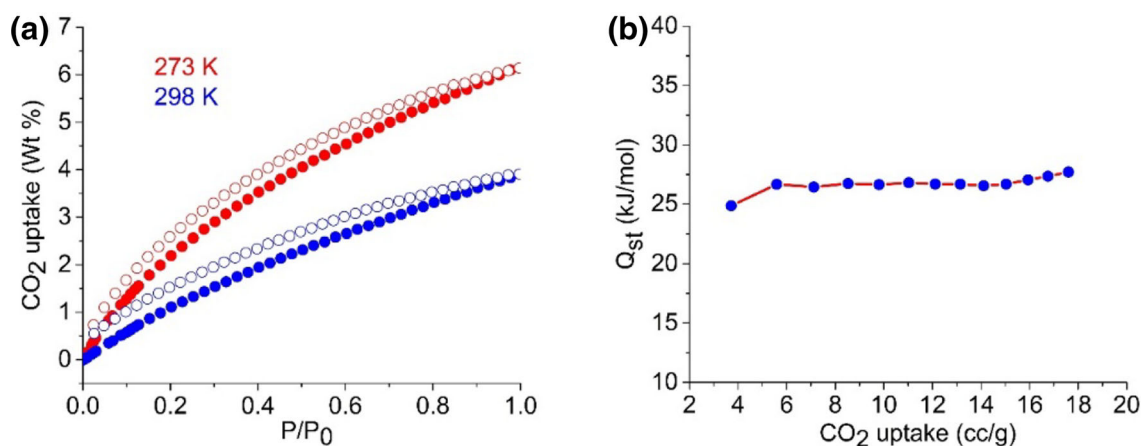

Figure 13. (a) CO_2 uptake at 273 and 298 K at 1 bar and (b) Isosteric heat of adsorption profile.

vicinity of –N=N- linkage, have shown better selectivity towards CO_2 due to the availability of –N=N- moieties for CO_2 to interact. However, in the present case, the bulky isopropyl substituents in the vicinity of –N=N- functionalities substantially reduce the interaction of the CO_2 with the polymer.[9]

For a better understanding of the CO_2 uptake, the isosteric heat of adsorption (Q_{st}) was calculated by fitting the adsorption data collected at 273 and 298 K by implementing Classius-Clayeperon equation. The Q_{st} value for ^{i}PrTAPB-Azo-COP at zero coverage was estimated to be 27.5 kJ mol^{-1} (Figure 13b), which is comparable to the values observed for previously reported azo-linked porous polymers (Table S2 in SI). Low-pressure CO_2 uptake studies of ^{i}PrTAPB-Azo-COP exhibits unsaturation at 1 bar. These results prompted us
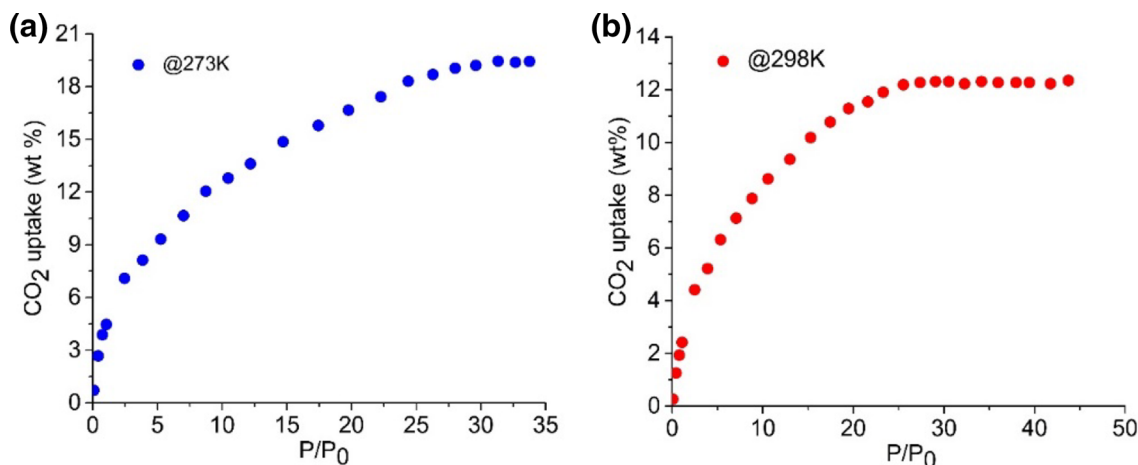
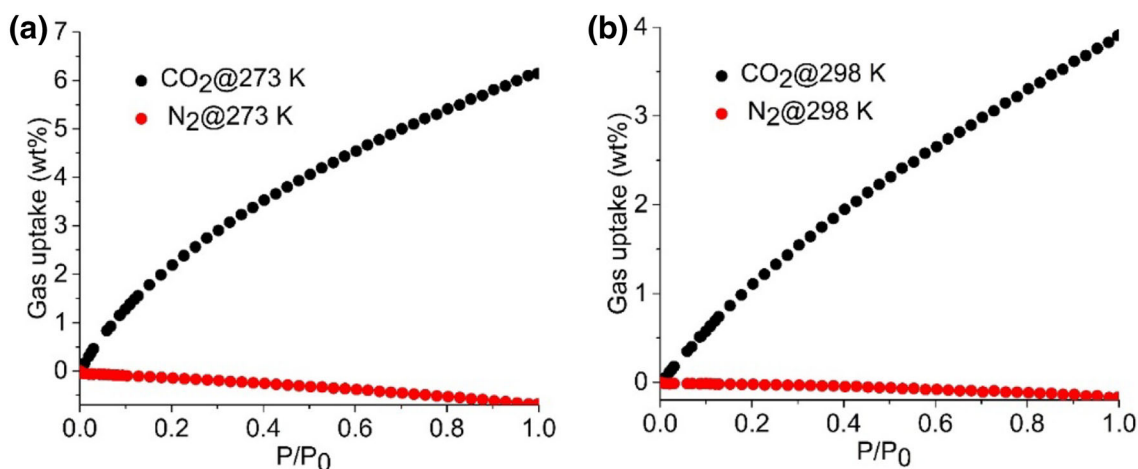**Figure 14.**   High-pressure CO_2 uptake (a) at 273 and (b) 298 K at 1 bar.

Figure 15. CO_2/N_2 selectivity (a) at 273 and (b) 298 K at 1 bar.

to investigate the high-pressure CO_2 uptake, resulting in 3 times increase in the CO_2 uptake capacity values. The CO_2 adsorption saturates at 19.6 wt% at 30 bar (273 K) and at 12.8 wt% at 25.0 bar (298 K) (Figure 14). Even though the bulky isopropyl groups flank the –N=N- functionalities in the polymer, ^{i}PrTAPB-Azo-COP exhibits higher selectivity towards CO_2 adsorption as compared to N_2 both at 273 and 298 K (Figure 15).

4.   Conclusions

In summary, we have synthesised and characterized a fluorescent triphenybenzene based azo-linked covalent organic polymer, ^{i}PrTAPB-Azo-COP, which is decorated with bulky isopropyl substituents. The COP exhibits excellent hydrolytic and chemical stability due to the presence of isopropyl groups and rigid azo linkages. ^{i}PrTAPB-Azo-COP exhibits significant BET surface area of 395 m^2g^{-1} and abundant microposity (9.6 Å) along with mesopores (37.0 Å). The band at

358 nm in the absorption spectrum of ^{i}PrTAPB-Azo-COP confirms the *trans*-orientation of the phenyl rings with respective to –N=N- linkages in the polymer network. The fluorescence spectrum of COP exhibits single broadband centred at 428 nm upon exciting at 300 nm and the intensity of the fluorescence was quenched by polynitroaromatic compounds (PNACs). Interestingly, PA has quenched the fluorescence at low concentration (13 ppm) compared to other PNACs. Owing to the CO_2-philic nature of azo functionality, ^{i}PrTAPB-Azo-COP exhibits CO_2 capture of about 6.5 wt% at 273 K and 1 bar but the CO_2 uptake was increased by 3 times (19.6 wt %) at higher pressure (30 bar and 273 K). Thus, it was concluded that fluorescent π-conjugated triphenylbenzene polymers/frameworks are potentially useful not only for detection of explosive but also in the area of other photo-electronic materials such as OLEDs and OFETs. It appears that an increase in CO_2-philic nitrogen content in the porous network would lead to higher CO_2 uptake. We are currently exploring these aspects.

Supplementary Information (SI)

CP-MAS ^{13}C NMR spectrum, comparison of PA's Stern-Volmer constant (K_{SV}) value of ^{i}PrTAPB-Azo-COP with small molecules, MOFs, COFs and COPs and comparison of surface area, CO_2 uptake and isosteric heat of adsorption (Q_{st}) of ^{i}PrTAPB-Azo-COP with various reported azo-linked polymers. Figure S1 and Tables S1 and S2 are available at www.ias.ac.in/chemsci.

Acknowledgements

References

1. (a) Nagarkar S S, Joarder B, Chaudhari A K, Mukherjee S and Ghosh S K 2013 Highly selective detection of nitro explosives by a luminescent metal–organic framework *Angew. Chem. Int. Edit.* **52** 2881; (b) Madhu S, Bandela A and Ravikanth M 2014 Bodipy based fluorescent chemodosimeter for explosive picric acid in aqueous media and rapid detection in the solid state *RSC Adv.* **4** 7120; (c) Dinda D, Gupta A, Shaw B K, Sadhu S and Saha S K 2014 Highly selective detection of trinitrophenol by luminescent functionalized reduced graphene oxide through fret mechanism *ACS Appl. Mater. Interfaces* **6** 10722; (d) He G, Peng H, Liu T, Yang M, Zhang Y and Fang Y 2009 A novel picric acid film sensor via combination of the surface enrichment effect of chitosan films and the aggregation-induced emission effect of siloles *J. Mater. Chem.* **19** 7347; (e) Roy B, Bar A K, Gole B and Mukherjee P S 2013 Fluorescent tris-imidazolium sensors for picric acid explosive *J. Org. Chem.* **78** 1306; (f) Sang N, Zhan C and Cao D 2015 Highly sensitive and selective detection of 2, 4, 6-trinitrophenol using covalent-organic polymer luminescent probes *J. Mater. Chem. A* **3** 92

2. (a) Ashbrook P C 2001 Elements of a role model hazardous waste management program for academic institutions *Chem. Health. Saf.* **8** 27; (b) Wollin K-M and Dieter H 2005 Toxicological guidelines for monocyclic nitro-, amino-and aminonitroaromatics, nitramines, and nitrate esters in drinking water *Arch. Environ. Contam. Toxicol.* **49** 18

3. (a) Håkansson K, Coorey R V, Zubarev R A, Talrose V L and Håkansson P 2000 Low-mass ions observed in plasma desorption mass spectrometry of high explosives *J. Mass Spectrom.* **35** 337; (b) Joarder B, Desai A V, Samanta P, Mukherjee S and Ghosh S K 2015 Selective and sensitive aqueous-phase detection of 2, 4, 6-trinitrophenol (tnp) by an amine-functionalized metal–organic framework *Chem. Eur. J.* **21** 965

4. Sohn H, Calhoun R M, Sailor M J and Trogler W C 2001 Detection of TNT and picric acid on surfaces and in seawater by using photoluminescent polysiloles *Angew. Chem. Int. Edit.* **40** 2104

5. (a) Yang J-S and Swager T M 1998 Fluorescent porous polymer films as TNT chemosensors: Electronic and structural effects *J. Am. Chem. Soc.* **120** 11864; (b) Shanmugaraju S, Jadhav H, Patil Y P and Mukherjee P S 2012 Self-assembly of an octanuclear platinum (II) tetragonal prism from a new pt$_4^{II}$ organometallic star-shaped acceptor and its nitroaromatic sensing study *Inorg. Chem.* **51** 13072

6. (a) Senthamizhan A, Celebioglu A and Uyar T 2015 Ultrafast on-site selective visual detection of TNT at sub-ppt level using fluorescent gold cluster incorporated single nanofiber *Chem. Commun.* **51** 5590; (b) Liu J, Yang S, Li F, Dong L, Liu J, Wang X and Pu Q 2015 Highly fluorescent polymeric nanoparticles based on melamine for facile detection of TNT in soil *J. Mater. Chem. A* **3** 10069; (c) Lin L, Rong M, Lu S, Song X, Zhong Y, Yan J, Wang Y and Chen X 2015 A facile synthesis of highly luminescent nitrogen-doped graphene quantum dots for the detection of 2, 4, 6-trinitrophenol in aqueous solution *Nanoscale* **7** 1872

7. (a) Bell T W and Hext N M 2004 Supramolecular optical chemosensors for organic analytes *Chem. Soc. Rev.* **33** 589; (b) Nambayah M and Quickenden T I 2004 A quantitative assessment of chemical techniques for detecting traces of explosives at counter-terrorist portals *Talanta* **63** 461; (c) Eiceman G and Stone J 2004 Peer reviewed: Ion mobility spectrometers in national defense *Anal. Chem.* **76** 390A; (d) Jiang Y, Zhao H, Zhu N, Lin Y, Yu P and Mao L 2008 A simple assay for direct colorimetric visualization of trinitrotoluene at picomolar levels using gold nanoparticles *Angew. Chem.* **120** 8729; (e) Zhou H, Zhang Z, Jiang C, Guan G, Zhang K, Mei Q, Liu R and Wang S 2011 Trinitrotoluene explosive lights up ultrahigh raman scattering of nonresonant molecule on a top-closed silver nanotube array *Anal. Chem.* **83** 6913; (f) Czarnik A W 1998 A sense for landmines *Nature* **394** 417

8. (a) Li J-S, Tang Y-J, Li S-L, Zhang S-R, Dai Z-H, Si L and Lan Y-Q 2015 Carbon nanodots functional MOFs composites by a stepwise synthetic approach: Enhanced H$_2$ storage and fluorescent sensing *CrystEngComm* **17** 1080; (b) Xie W, Zhang S-R, Du D-Y, Qin J-S, Bao S-J, Li J, Su Z-M, He W-W, Fu Q and Lan Y-Q 2015 Stable luminescent metal–organic frameworks as dual-functional materials to encapsulate Ln^{3+} ions for white-light emission and to detect nitroaromatic explosives *Inorg. Chem.* **54** 3290; (c) Bandela A K, Bandaru S and Rao C P 2015 A fluorescent 1, 3-diaminonaphthalimide conjugate of calix [4] arene for sensitive and selective detection of trinitrophenol: Spectroscopy, microscopy, and computational studies, and its applicability using cellulose strips *Chem. Eur. J.* **21** 13364; (d) Venkatramaiah N, Kumar S and Patil S 2012 Fluoranthene based fluorescent chemosensors for detection of explosive nitroaromatics *Chem. Commun.* **48** 5007

9. (a) Chopra R, Kaur P and Singh K 2015 Pyrene-based chemosensor detects picric acid upto attogram level through aggregation enhanced excimer emission *Anal. Chim. Acta* **864** 55; (b) Udhayakumari D, Velmathi S, Venkatesan P and Wu S-P 2015 A pyrene-linked thiourea

as a chemosensor for cations and simple fluorescent sensor for picric acid *Anal. Methods* **7** 1161; (c) Gupta S K, Kaleeswaran D, Nandi S, Vaidhyanathan R and Murugavel R 2017 Bulky isopropyl group loaded tetraaryl pyrene based azo-linked covalent organic polymer for nitroaromatics sensing and CO_2 adsorption *ACS Omega* **2** 3572

10. Durga Prasad K, Venkataramaiah N and Guru Row T N 2014 1, 9-pyrazoloanthrone as a colorimetric and "turn-on" fluorometric chemosensor: Structural implications *Cryst. Growth Des.* **14** 2118

11. (a) Peng Y, Zhang A-J, Dong M and Wang Y-W 2011 A colorimetric and fluorescent chemosensor for the detection of an explosive—2, 4, 6-trinitrophenol (TNP) *Chem. Commun.* **47** 4505; (b) Neena K K and Thilagar P 2016 Replacing the non-polarized C=C bond with an isoelectronic polarized B–N unit for the design and development of smart materials *J. Mater. Chem. C* **4** 11465

12. Kartha K K, Sandeep A, Praveen V K and Ajayaghosh A 2015 Detection of nitroaromatic explosives with fluorescent molecular assemblies and π − gels *Chem. Rec.* **15** 252

13. (a) Shaw P E, Chen S S, Wang X, Burn P L and Meredith P 2013 High-generation dendrimers with excimer-like photoluminescence for the detection of explosives *J. Phys. Chem. C* **117** 5328; (b) Shoaee S, Chen S S, Cavaye H, Smith A R, Burn P L, Gentle I R, Meredith P and Shaw P E 2017 Assessing the sensing limits of fluorescent dendrimer thin films for the detection of explosive vapors *Sens. Actuators B-Chem.* **239** 727

14. (a) Hong G, Sun J, Qian C, Xue P, Gong P, Zhang Z and Lu R 2015 Nanofibers generated from linear carbazole-based organogelators for the detection of explosives *J. Mater. Chem. C* **3** 2371; (b) Xu Y, Wu X, Chen Y, Hang H, Tong H and Wang L 2016 Star-shaped triazatruxene derivatives for rapid fluorescence fiber-optic detection of nitroaromatic explosive vapors *RSC Adv.* **6** 31915; (c) Kaleeswaran D, Vishnoi P, Kumar S, Chithiravel S, Walawalkar M G, Krishnamoorthy K and Murugavel R 2016 Alkyl-chain-separated triphenybenzene-carbazole conjugates and their derived polymers: Candidates for sensory, electrical and optical materials *ChemistrySelect* **1** 6649; (d) Mei X, Wei K, Wen G, Liu Z, Lin Z, Zhou Z, Huang L, Yang E and Ling Q 2016 Carbazole-based diphenyl maleimides: Multi-functional smart fluorescent materials for data process and sensing for pressure, explosive and ph *Dyes Pigments* **133** 345; (e) Prakash K and Nagarajan R 2013 Synthesis of solid state fluorescent quino [2, 3-b] carbazoles via copper (II) triflate-catalyzed heteroannulation: Application to detection of TNT *Tetrahedron* **69** 8269

15. Shanmugaraju S and Mukherjee P S 2015 Π-electron rich small molecule sensors for the recognition of nitroaromatics *Chem. Commun.* **51** 16014

16. Xu S and Lu H 2015 Ratiometric fluorescence and mesoporous structure dual signal amplification for sensitive and selective detection of tnt based on MIP@QD fluorescence sensors *Chem. Commun.* **51** 3200

17. (a) Zhou H, Ye Q, Neo W T, Song J, Yan H, Zong Y, Tang B Z, Hor T A and Xu J 2014 Electrospun aggregation-induced emission active poss-based porous copolymer films for detection of explosives *Chem. Commun.* **50** 13785; (b) Ma X, Tao F, Zhang Y, Li T, Raymo F M and Cui Y 2017 Detection of nitroaromatic explosives by 3D hyperbranched $\sigma - \pi$ conjugate polymer on the basis of the poss scaffold *J. Mater. Chem. A* **5** 14343

18. (a) Chowdhury A, Howlader P and Mukherjee P S 2016 Aggregation-induced emission of platinum (II) metallacycles and their ability to detect nitroaromatics *Chem. Eur. J.* **22** 7468; (b) Sandhu S, Kumar R, Singh P and Kumar S 2016 Impact of aggregation on fluorescence sensitivity of molecular probes towards nitroaromatic compounds *J. Mater. Chem. C* **4** 3209; (c) Zwijnenburg M A, Berardo E, Peveler W J and Jelfs K E 2016 Amine molecular cages as supramolecular fluorescent explosive sensors: A computational perspective *J. Phys. Chem. B* **120** 5063

19. (a) Hu Z, Deibert B J and Li J 2014 Luminescent metal–organic frameworks for chemical sensing and explosive detection *Chem. Soc. Rev.* **43** 5815; (b) Nagarkar S S, Desai A V and Ghosh S K 2016 Engineering metal–organic frameworks for aqueous phase 2, 4, 6-trinitrophenol (TNP) sensing *CrystEngComm* **18** 2994; (c) Yang Y, Shen K, Lin J-Z, Zhou Y, Liu Q-Y, Hang C, Abdelhamid H N, Zhang Z-Q and Chen H 2016 A Zn-MOF constructed from electron-rich π-conjugated ligands with an interpenetrated graphene-like net as an efficient nitroaromatic sensor *RSC Adv.* **6** 45475; (d) Yadav A, Deshmukh M S and Boomishankar R 2017 Cationic and neutral copper (I) iodide cluster MOFs derived from tridentate N-donor functionalized P(V) ligands: Synthesis, structure and photophysical properties *J. Chem. Sci.* **129** 1093; (e) Santra A, Francis M, Parshamoni S and Konar S 2017 Nanoporous Cu(I) metal–organic framework: Selective adsorption of benzene and luminescence sensing of nitroaromatics *ChemistrySelect* **2** 3200; (f) Sanda S, Parshamoni S, Biswas S and Konar S 2015 Highly selective detection of palladium and picric acid by a luminescent MOF: A dual functional fluorescent sensor *Chem. Commun.* **51** 6576; (g) Parshamoni S, Telangae J and Konar S 2015 Regulation of the pore size by shifting the coordination sites of ligands in two MOFs: Enhancement of CO_2 uptake and selective sensing of nitrobenzene *Dalton Trans.* **44** 20926

20. (a) Das G, Biswal B P, Kandambeth S, Venkatesh V, Kaur G, Addicoat M, Heine T, Verma S and Banerjee R 2015 Chemical sensing in two dimensional porous covalent organic nanosheets *Chem. Sci.* **6** 3931; (b) Kaleeswaran D, Vishnoi P and Murugavel R 2015 [3+ 3] imine and β-ketoenamine tethered fluorescent covalent-organic frameworks for CO_2 uptake and nitroaromatic sensing *J. Mater. Chem. C* **3** 7159; (c) Dalapati S, Jin S, Gao J, Xu Y, Nagai A and Jiang D 2013 An azine-linked covalent organic framework *J. Am. Chem. Soc.* **135** 17310

21. McCluskey A, Holdsworth C I and Bowyer M C 2007 Molecularly imprinted polymers (MIPs): Sensing, an explosive new opportunity? *Org. Bio. Chem.* **5** 3233

22. (a) Guo L and Cao D 2015 Color tunable porous organic polymer luminescent probes for selective sensing of metal ions and nitroaromatic explosives *J. Mater. Chem. C* **3** 8490; (b) Bhunia A, Esquivel D, Dey S,

Fernández-Terán R, Goto Y, Inagaki S, Van Der Voort P and Janiak C 2016 A photoluminescent covalent triazine framework: CO_2 adsorption, light-driven hydrogen evolution and sensing of nitroaromatics *J. Mater. Chem. A* **4** 13450; (c) Deshmukh A, Bandyopadhyay S, James A and Patra A 2016 Trace level detection of nitroanilines using a solution processable fluorescent porous organic polymer *J. Mater. Chem. C* **4** 4427; (d) Sun X, Wang Y and Lei Y 2015 Fluorescence based explosive detection: From mechanisms to sensory materials *Chem. Soc. Rev.* **44** 8019

23. (a) Thomas S W, Joly G D and Swager T M 2007 Chemical sensors based on amplifying fluorescent conjugated polymers *Chem. Rev.* **107** 1339; (b) Yang J-S and Swager T M 1998 Porous shape persistent fluorescent polymer films: An approach to tnt sensory materials *J. Am. Chem. Soc.* **120** 5321

24. (a) Gomes R, Bhanja P and Bhaumik A 2015 A triazine-based covalent organic polymer for efficient CO_2 adsorption *Chem. Commun.* **51** 10050; (b) Chakraborty S, Colón Y J, Snurr R Q and Nguyen S T 2015 Hierarchically porous organic polymers: Highly enhanced gas uptake and transport through templated synthesis *Chem. Sci.* **6** 384; (c) Nandi S, Werner-Zwanziger U and Vaidhyanathan R 2015 A triazine–resorcinol based porous polymer with polar pores and exceptional surface hydrophobicity showing CO_2 uptake under humid conditions *J. Mater. Chem. A* **3** 21116; (d) Nandi S, Rother J, Chakraborty D, Maity R, Werner-Zwanziger U and Vaidhyanathan R 2017 Exceptionally stable bakelite-type polymers for efficient pre-combustionCO_2 capture and H_2 purification *J. Mater. Chem. A* **5** 8431

25. (a) Zhang Y and Riduan S N 2012 Functional porous organic polymers for heterogeneous catalysis *Chem. Soc. Rev.* **41** 2083; (b) Seo M, Kim S, Oh J, Kim S-J and Hillmyer M A 2015 Hierarchically porous polymers from hyper-cross-linked block polymer precursors *J. Am. Chem. Soc.* **137** 600; (c) Dogru M, Handloser M, Auras F, Kunz T, Medina D, Hartschuh A, Knochel P and Bein T 2013 A photoconductive thienothiophene-based covalent organic framework showing charge transfer towards included fullerene *Angew. Chem.* **125** 2992; (d) Bildirir H, Gregoriou V G, Avgeropoulos A, Scherf U and Chochos C L 2017 Porous organic polymers as emerging new materials for organic photovoltaic applications: Current status and future challenges *Mater. Horiz.* **4** 546; (e) Peng P, Zhou Z, Guo J and Xiang Z 2017 Well-defined 2d covalent organic polymers for energy electrocatalysis *ACS Energy Lett.* **2** 1308; (f) Wu D, Xu F, Sun B, Fu R, He H and Matyjaszewski K 2012 Design and preparation of porous polymers *Chem. Rev.* **112** 3959; (g) Xu Y, Jin S, Xu H, Nagai A and Jiang D 2013 Conjugated microporous polymers: Design, synthesis and application *Chem. Soc. Rev.* **42** 8012; (h) Mukherjee G, Thote J, Aiyappa H B, Kandambeth S, Banerjee S, Vanka K and Banerjee R 2017 A porous porphyrin organic polymer (PPOP) for visible light triggered hydrogen production *Chem. Commun.* **53** 4461; (i) Rao K V, Haldar R, Maji T K and George S J 2016 Dynamic, conjugated microporous polymers: Visible light harvesting via guest-responsive reversible swelling *Phys. Chem. Chem. Phys.* **18** 156; (j) Suresh V M, Bandyopadhyay A, Roy S, Pati S K and Maji T K 2015 Highly luminescent microporous organic polymer with lewis acidic boron sites on the pore surface: Ratiometric sensing and capture of F-ions *Chem. Eur. J.* **21** 10799

26. (a) Haszeldine R S 2009 Carbon capture and storage: How green can black be? *Science* **325** 1647; (b) Rochelle G T 2009 Amine scrubbing for CO_2 capture *Science* **325** 1652

27. (a) Patel H A, Je S H, Park J, Chen D P, Jung Y, Yavuz C T and Coskun A 2013 Unprecedented high-temperature CO_2 selectivity in N_2-phobic nanoporous covalent organic polymers *Nat. Commun.* **4** 1357; (b) Arab P, Rabbani M G, Sekizkardes A K, İslamoğlu T and El-Kaderi H M 2014 Copper (I)-catalyzed synthesis of nanoporous azo-linked polymers: Impact of textural properties on gas storage and selective carbon dioxide capture *Chem. Mater.* **26** 1385; (c) Ashourirad B, Sekizkardes A K, Altarawneh S and El-Kaderi H M 2015 Exceptional gas adsorption properties by nitrogen-doped porous carbons derived from benzimidazole-linked polymers *Chem. Mater.* **27** 1349; (d) Rabbani M G and El-Kaderi H M 2012 Synthesis and characterization of porous benzimidazole-linked polymers and their performance in small gas storage and selective uptake *Chem. Mater.* **24** 1511; (e) Rabbani M G, Sekizkardes A K, Kahveci Z, Reich T E, Ding R and El-Kaderi H M 2013 A 2D mesoporous imine-linked covalent organic framework for high pressure gas storage applications *Chem. Eur. J.* **19** 3324; (f) Sekizkardes A K, Altarawneh S, Kahveci Z, İslamoğlu T and El-Kaderi H M 2014 Highly selective CO_2 capture by triazine-based benzimidazole-linked polymers *Macromolecules* **47** 8328; (g) Byun J, Je S-H, Patel H A, Coskun A and Yavuz C T 2014 Nanoporous covalent organic polymers incorporating Tröger's base functionalities for enhanced CO_2 capture *J. Mater. Chem. A* **2** 12507

28. Islamoglu T, Kim T, Kahveci Z, El-Kadri O M and El-Kaderi H M 2016 Systematic postsynthetic modification of nanoporous organic frameworks for enhanced CO_2 capture from flue gas and landfill gas *J. Phys. Chem. C* **120** 2592

29. (a) Nagendran S, Vishnoi P and Murugavel R 2017 Triphenylbenzene sensor for selective detection of picric acid *J. Fluoresc.* **27** 1299; (b) Vishnoi P, Sen S, Patwari G N and Murugavel R 2015 Charge transfer aided selective sensing and capture of picric acid by triphenylbenzenes *New J. Chem.* **39** 886; (c) Vishnoi P, Walawalkar M G and Murugavel R 2014 Containment of polynitroaromatic compounds in a hydrogen bonded triarylbenzene host *Cryst. Growth Des.* **14** 5668; (d) Vishnoi P, Walawalkar M G, Sen S, Datta A, Patwari G N and Murugavel R 2014 Selective fluorescence sensing of polynitroaromatic explosives using triaminophenylbenzene scaffolds *Phys. Chem. Chem. Phys.* **16** 10651

30. Kaleeswaran D, Antony R, Sharma A, Malani A and Murugavel R 2017 Catalysis and CO_2 capture by palladium incorporated covalent organic frameworks *ChemPlusChem* **82** 1253

31. Armarego W L and Chai C L L 2009 Purification of laboratory chemicals (Oxford: Butterworth-Heinemann) p. 88

32. (a) Patel H A, Je S H, Park J, Jung Y, Coskun A and Yavuz C T 2014 Directing the structural features of N_2-phobic nanoporous covalent organic polymers for CO_2 capture and separation *Chem. Eur. J.* **20** 772; (b) Yang Z, Zhang H, Yu B, Zhao Y, Ma Z, Ji G, Han B and Liu Z 2015 Azo-functionalized microporous organic polymers: Synthesis and applications in CO_2 capture and conversion *Chem. Commun.* **51** 11576; (c) Lu J and Zhang J 2014 Facile synthesis of azo-linked porous organic frameworks via reductive homocoupling for selective CO_2 capture *J. Mater. Chem. A* **2** 13831

33. Arab P, Parrish E, İslamoğlu T and El-Kaderi H M 2015 Synthesis and evaluation of porous azo-linked polymers for carbon dioxide capture and separation *J. Mater. Chem. A* **3** 20586

34. (a) Mostakim S and Biswas S 2016 A thiadiazole-functionalized Zr(IV)-based metal–organic framework as a highly fluorescent probe for the selective detection of picric acid *CrystEngComm* **18** 3104; (b) Chahal M K and Sankar M 2015 1, 8-naphthyridine-based fluorescent receptors for picric acid detection in aqueous media *Anal. Methods* **7** 10272; (c) Mukherjee S, Desai A V, Manna B, Inamdar A I and Ghosh S K 2015 Exploitation of guest accessible aliphatic amine functionality of a metal–organic framework for selective detection of 2, 4, 6-trinitrophenol (TNP) in water *Cryst. Growth Des.* **15** 4627; (d) Mutneja R, Singh R, Kaur V, Wagler J, Kroke E and Kansal S K 2017 Proton transfer assisted facile encapsulation of picric acid in sol-gel derived silica decorated with azo-azomethine hosts *Dyes Pigments* **139** 635

35. Zhang Y, Zhu Y, Guo J, Gu S, Wang Y, Fu Y, Chen D, Lin Y, Yu G and Pan C 2016 The role of the internal molecular free volume in defining organic porous copolymer properties: Tunable porosity and highly selective CO_2 adsorption *Phys. Chem. Chem. Phys.* **18** 11323

36. Tao L, Niu F, Zhang D, Liu J, Wang T and Wang Q 2015 Azo-bridged covalent porphyrinic polymers (Azo-CPPs): Synthesis and CO_2 capture properties *RSC Adv.* **5** 96871